Oxygen vacancies and defect electronic states on the $SnO_2(110)$-1×1 surface

David F. Cox,* Teresa B. Fryberger, and Steve Semancik
Chemical Process Metrology Division, National Bureau of Standards, Gaithersburg, Maryland 20899
(Received 6 January 1988)

The $SnO_2(110)$-1×1 surface, a surface which is structurally similar to the more studied $TiO_2(110)$ surface, has been found to be an ideal system of study for the identification and characterization of surface oxygen vacancies. Heating a well-oxidized, nearly perfect (110) surface in UHV removes large amounts of surface lattice oxygen. Ion-scattering spectroscopy (ISS) and ultraviolet photoelectron spectroscopy (UPS) have shown conclusively that defect electronic states which appear low in the band gap for annealing temperatures less than 800 K arise from "bridging" oxygen vacancies [i.e., from the removal of oxygen anions from the terminal layer of an ideal, rutile-structure (110) surface]. UPS and four-point conductivity measurements indicate that heating at 800 K or above causes the formation of a second type of surface defect. It is argued that this second defect is an "in-plane" oxygen vacancy [i.e., the result of removing an oxygen anion from what is normally the second, tin-containing, atomic plane of an ideal (110) surface]. The in-plane oxygen vacancy is characterized by occupied states higher in the band gap which extend to the Fermi level.

I. INTRODUCTION

The surface electronic structure of metal-oxide materials plays an important role in their use in many technologically important areas such as catalysis, chemical gas sensing, and microelectronics. The occurrence of intrinsic surface states and the origin and nature of extrinsic defect states are, therefore, properties of practical and fundamental interest. One problem encountered in the characterization of metal-oxide surfaces is the difficulty in preparing ideal or nearly ideal single-crystal surfaces. Vacuum cleavage is the preferred method for preparing ideal surfaces,[1] but this technique may be impractical if the sample is small and fragile. Another difficulty is encountered in reproducibly creating and characterizing surface defects. Heating and electron or low-energy ion bombardment of oxides are used often to create surface defects, but these methods typically do not allow for the *controlled* creation and characterization of single types of surface defects. Because of these characterization problems it has proven difficult in most cases to directly relate observed electronic states with specific types of defect sites.

In this paper, the electronic properties of oxygen vacancies on the $SnO_2(110)$-1×1 surface are examined in detail. Two different types of oxygen vacancies are identified, and separate band-gap electronic states are shown for each. Ion scattering spectroscopy (ISS) proved to be very useful as both a compositional and structural probe in obtaining these findings. Ultraviolet photoelectron spectroscopy (UPS) was used as the primary probe of surface electronic structure, and four-point probe conductivity measurements were applied as a complementary method for investigating effects that originate from portions of the electronic structure with too small an occupancy to be observed in UPS.

II. BACKGROUND

SnO_2 is an n-type, wide-band-gap ($E_g=3.6$ eV) semiconductor with the rutile (TiO_2) structure. When viewed along the [110] direction, the crystal is seen to be composed of charge-neutral "units," each containing three atomic planes.[2] The composition and arrangement of the three planes in the "unit" are $[(O^{2-})(2Sn^{4+}+2O^{2-})(O^{2-})]$ per (110) unit cell. The charge on each plane is therefore $[(2-)(4+)(2-)]$, and the net charge per "unit" is zero. An ideal, stoichiometric (110) surface is terminated by a charge-neutral unit, and because this unit has no net dipole moment in the [110] direction the (110) surface is nonpolar. Terminating the (110) surface with a complete, nonpolar, charge-neutral unit corresponds to breaking the smallest number of cation-anion bonds relative to the bulk structure.[1] This termination results in fivefold- and sixfold-coordinated surface cations in equal numbers. The full bulk coordination per cation is six. Figure 1 is a ball model illustration of the ideal, stoichiometric $SnO_2(110)$ surface based on the ionic radii of Sn^{4+} and O^{2-} ions. From Fig. 1 and the preceding discussion it is clear that the ideal (110) surface is terminated with an outermost plane of oxygen atoms which appear as rows in the [001] direction and occupy bridging positions between the second-layer sixfold-coordinated tin atoms. Oxygen atoms in the second layer may also be seen in Fig. 1 in the same plane as the observable tin atoms. For convenience, these two different types of oxygen anions will be referred to as "bridging" oxygens and "in-plane" oxygens, respectively.

The most detailed surface studies of $SnO_2(110)$ reported to date are those of deFrésart and co-workers,[3] which examine the thermally driven reconstructions of ion-bombarded surfaces with Auger-electron spectroscopy

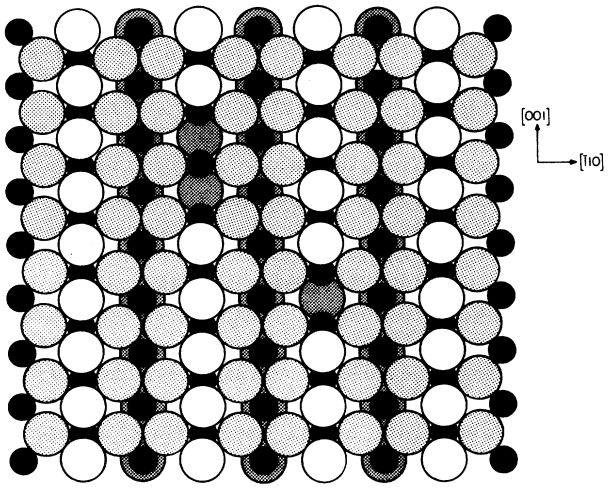

FIG. 1. Ball model illustration of a nearly perfect (ideal) $SnO_2(110)$ surface based on the ionic radii of the ions. The small solid circles represent Sn^{4+} cations, while the large open circles represent O^{2-} anions. All the visible tin cations are in the second atomic layer. Increased shading of the oxygen anions represents increased depth away from the surface. Several "bridging" oxygen anions have been removed from the terminal layer to represent oxygen vacancies and to give a clearer view of the (normally) sixfold-coordinated tin cations in the second layer.

(AES), low-energy electron diffraction (LEED), low-energy electron-loss spectroscopy (LEELS), and sheet conductance measurements. They found a correlation between composition as measured by AES and surface conductivity from four-point sheet resistivity measurements; high values of sheet conductance were typically associated with low [O]/[Sn] ratios. A number of different surface reconstructions were observed as a function of heating temperature; (4×1), $c(1\times1)$, (1×1), (1×2), and (2×1) LEED periodicities were identified. The different LEED periodicities were explained in terms of ordered patterns of surface oxygen vacancies.

A more recent LEED and AES study has also been performed on the $SnO_2(110)$ surface.[4] Most of the LEED periodicities observed by deFrésart and coworkers[3] were seen with the exception of the (2×1) patterns. While the patterns have been interpreted differently than in the original study, the proposed structures are all based on oxygen-deficient surfaces. Sheet conductance measurements have also been reported recently by Erickson and Semancik for the $SnO_2(110)$ surface.[5] The primary conclusion to be drawn from these studies is that oxygen vacancies or oxygen deficiencies on the (110) surface can increase the surface conductivity by more than two orders of magnitude with respect to the bulk conductivity. It is well known that oxygen vacancies in the bulk act as *n*-type donors,[6,7] and these surface studies demonstrate a similar behavior for surface oxygen vacancies.

While a significant amount of photoemission work is available on the $SnO_2(001)$ surface,[8] less complete results have been reported for the (110) surface.[9–12] Egdell *et al.*[9] have reported UPS spectra for oxidized and ion-bombarded (110) surfaces, and several reports of UPS studies of the thermally driven reconstructions and the interaction of O_2, H_2, and H_2O with the (110) surface have also been published.[10–12] These studies show that the oxygen deficient $SnO_2(110)$ surface displays a significant density of surface states in the band gap up to the Fermi level, but oxidized (i.e., more ideal) surfaces show no significant density of band-gap states. Also, evidence has been found suggesting that adsorbates show a specificity for different defect (oxygen vacancy-derived) electronic states in the band gap.[11] P. A. Cox *et al.*[2] and Egdell *et al.*[9] have suggested that defect states near the valence-band maximum (VBM) are due to a rehybridization of Sn $5s$-$5p$ states at reduced Sn^{2+} sites adjacent to oxygen vacancies or in local SnO-like environments at the surface.

Several theoretical studies of the bulk and surface electronic structure of SnO_2 have appeared in the literature.[13–16] The most successful theoretical bulk study appears to be the tight-binding calculation of Robertson[15(a)] which predicts a VBM with Γ_3^+ symmetry and a conduction-band minimum (CBM) with Γ_1^+ symmetry in agreement with experiment. Robertson has also examined the electronic properties of different bulk defects using the tight-binding Green's-function method.[15(b)] He calculates that the defect donor levels associated with an unrelaxed oxygen vacancy (V_O) fall above the CBM, while V_O^+ is shallow in the gap with the single defect electron bound by the Coulombic well of the positively charged vacancy. V_O^+ may therefore be viewed as an E' center (i.e., an oxygen vacancy binding an electron) in SnO_2. Note that experimentally, Samson and Fonstad[7] found both V_O and V_O^+ donors to be shallow in the gap. They report a first and second ionization potential for V_O of 0.030 and 0.150 eV, respectively.[7]

The electronic structure of several low index faces of SnO_2 has also been studied by Munnix and Schmeits using the scattering-theoretical method.[16] While their results predict a number of surface resonances in the valence and conduction bands, they do not predict any surface states in the band gap. In Ref. 16(d), they specifically consider a number of different types of unrelaxed tin and oxygen vacancies on the $SnO_2(110)$ surface, but no band-gap states are predicted. This result is clearly contradicted by the available experimental data on the (110) surface[9–12] as well as the data from this work. Egdell *et al.*[9] have suggested that the discrepancy may be due to relaxation about the vacancies, but no experimental data is available concerning surface relaxations of ideal or defective SnO_2 surfaces.

III. EXPERIMENT

The sample used for this study was cut from the side of a hollow, needle-shaped SnO_2 single crystal grown by the vapor-phase reaction method.[17] The crystal was oriented by Laue backreflection and mechanically polished to within 1° of the (110) surface. The resulting sample was approximately $7\times3\times\frac{1}{4}$ mm^3. The bulk conductivity of the sample at room temperature was about 10^{-7} $\Omega^{-1}\,\mathrm{cm}^{-1}$.[18] The very small thickness of the sample

made the vacuum cleavage method of preparing the surface impractical.

The sample was clamped to a small tantalum holder which provided mechanical stability, and acted as both an electrical contact and a resistive heater. The holder was supported by two 1-mm-diameter tantalum wires held firmly against the holder by small stainless steel screws and washers. These wires acted as electrical leads for the resistive heating. A W–5 at. % Re/W–26 at. % Re thermocouple was spotwelded to the back of the holder for temperature measurements. This arrangement did not provide a direct measure of the sample temperature, but it was assumed that the sample came to thermal equilibrium with the holder during heating cycles.

Argon-ion bombardment and heating were used to clean and order the surface of the $SnO_2(110)$ crystal, and its condition was monitored by x-ray photoelectron spectroscopy (XPS). None of the surface preparations reported here led to the formation of metallic tin (Sn^0) in concentrations observable by XPS. All gas exposures were performed in an UHV preparation chamber by backfilling through a variable leak valve. The sample was directly transported between the connected preparation and analysis chambers on a long-stroke manipulator. *In situ* four-point probe conductivity measurements were made with an UHV compatible device which is described in detail elsewhere.[19] Low-energy electron diffraction measurements were made with LEED-ESDIAD (electron-stimulated desorption ion angular distribution) charged-particle imaging optics.[20] UPS and ISS measurements were made in the analysis chamber with a commercial hemispherical analyzer. For UPS measurements, a rf gas discharge lamp was used as a source of He I radiation ($h\nu=21.2$ eV), and the analyzer resolution was set at 0.15 eV. Each UPS spectrum was corrected for the presence of weak lines at 23.1 eV (2.3%) and 23.7 eV (0.7%) in order to determine the density of states in the band gap as accurately as possible. The relative contributions of the weak lines and the position of the Fermi level were determined from a thick Pd overlayer deposited on the sample at the end of the study. All UPS and four-point conductivity measurements were made at 300 K. For the ISS measurements, also made near 300 K, a scattering angle of 130° was set by the fixed positions of the ion source and the analyzer. An incident He^+ ion beam with a primary energy (E_0) of 1000 eV and 10 nA current level was used at an incident angle of 50° with respect to the surface normal along the [001] azimuth. The base pressure for this study was 5×10^{-11} Torr in the analysis chamber and 8×10^{-11} Torr in the preparation chamber. A complete description of the experimental apparatus is given elsewhere.[21]

IV. RESULTS AND DISCUSSION

A. Surface variability with pretreatment

It is widely recognized that the properties of oxide surfaces can be highly variable and strongly history dependent.[1,22] This variability often is connected to differences in the concentration of surface defects such as anion and cation vacancies or interstitials. SnO_2, for example, is conductive because of bulk and surface oxygen vacancies. In this experimental study, an attempt has been made to control the variability by oxidizing the surface *in situ*. High-pressure (about 1 Torr) and high-temperature oxidation treatments result in a nearly ideal $SnO_2(110)$ surface as will be shown below, and represent a useful method for obtaining a reproducible starting point for the experimental examination of the properties of surface defects on SnO_2. Direct comparisons of the various surfaces formed by oxidation and heating in vacuum allow a detailed description to be given of the chemical, structural, and electronic nature of oxygen vacancies on the $SnO_2(110)$-1×1 surface.

The variability of the surface oxygen concentration on sample history is summarized in terms of [O]/[Sn] ratios in Table I. Data are given for three different surface preparations: (1) bombardment with 2-keV Ar ions, (2) annealing at 1000 K in vacuum after bombardment, and (3) oxidation at 700 K in 1 Torr of O_2 after treatments (1) and (2). The XPS results represent ratios of the areas under the oxygen 1*s* and tin $3d_{5/2}$ peaks, and the ISS results are calculated from the integrated intensities of the scattering signals for oxygen and tin. Note that the true experimental ratios are different for ISS and XPS because of the different sampling depths and elemental cross sections of the two techniques. For the sake of comparison, both sets of data in Table I have been normalized with respect to the oxidized surface. From Table I it is seen that the surface oxygen-to-tin ratio increases in the following order of surface preparations: ion bombarded, 1000-K vacuum anneal, oxidized. No metallic tin (Sn^0) is observed in XPS for any of these surface preparations. When examined with LEED, the ion-bombarded surface exhibited only a diffuse background with no observable LEED beams. The other two surfaces both exhibited (1×1) LEED patterns which have the same periodicity as that expected for a simple termination of the bulk structure.

The low [O]/[Sn] ratio observed for the ion-bombarded surface is consistent with other studies which demonstrate that oxygen is preferentially sputtered from the $SnO_2(110)$ surface during argon-ion bombardment.[3,4] Annealing the bombarded surface to sufficiently high temperatures in vacuum results in surface ordering and reoxidation by diffusion of oxygen from the bulk.[3,4] Depending on the annealing temperature, a number of different surface reconstructions can be observed with LEED. It has been found that temperatures of about 600 K are sufficiently high to allow for the diffusion of excess

TABLE I. Variation in normalized [O]/[Sn] ratio with surface treatment.

Surface condition	XPS ([O]/[Sn])	ISS ([O]/[Sn])
700 K, 1 Torr O_2 oxidation	1.0	1.0
1000-K anneal in vacuum after ion bombardment	0.95	0.17
Ion bombarded	0.77	0.06

tin cations in the sputtered layer to reconstruct into their nominal bulk arrangement at the surface. The thermally driven reconstruction process and different periodicities observed in LEED are discussed in detail elsewhere.[4] For the present discussion, an annealing temperature was purposely chosen which gives a surface with a (1×1) LEED periodicity. The data in Table I indicate, therefore, that it is possible to form surfaces which nominally exhibit the bulk structure like an ideal surface, but which are significantly oxygen deficient in comparison to the ideal, stoichiometric surface. Note that the trends in the XPS and ISS data in Table I are similar, but the degree of variation in the [O]/[Sn] ratio is much higher for the ISS data. This variation may be understood in terms of the different sampling depths of the two techniques. XPS samples a larger concentration of bulk or subsurface oxygen from the SnO_2 matrix, while ISS with its nearly top layer sensitivity emphasizes the large variations in surface oxygen concentration which are possible with different preparation conditions. The ISS data give a particularly revealing comparison between the annealed and oxidized surface. Both surfaces exhibit a (1×1) LEED pattern with a periodicity characteristic of the bulk structure, but the ISS data demonstrate the significant compositional variation associated with these ordered surfaces. The ISS data indicate that a simple sputter-anneal treatment cannot produce an ideal, stoichiometric surface.

The variability in surface composition illustrated in Table I has a strong effect on the electronic states which appear in the band gap of SnO_2. Figure 2 shows UPS spectra for the three surface preparations which coincide with the data in Table I. A full valence-band spectrum for each surface preparation is indicated, as well as an enlarged view of the emission in the band-gap region. Longer counting times were used for the upper valence-band and band-gap regions to enhance the signal-to-noise ratio of the data.

The spectrum for the oxidized surface shows the highest valence-band density of states of the three spectra. The largest peak in the density of states occurs at a binding energy of 4.4 eV relative to the Fermi level. The intensity of this feature is directly correlated with the surface oxygen concentration as measured by AES,[4] XPS, and ISS (Table I). In general, the higher the surface oxygen concentration, the higher the peak intensity in UPS. This observation is in agreement with both bulk[15(a)] and surface[16] band-structure calculations which show that the feature is due primarily to oxygen $2p$ lone-pair-like states. The valence-band features at higher binding energies are composed of bands which exhibit hybridized O $2p$–Sn $5s$ and O $2p$–Sn $5p$ character.[15(a),16] The intensity of these features also varies with surface oxygen concentration but to a lesser degree than the O $2p$ lone-pair states.

From Fig. 2 it can be seen that the two surfaces showing the lowest valence-band density of states (i.e., the ion-bombarded and vacuum-annealed surfaces) exhibit the highest occupied density of states in the band-gap region. In both cases the emission extends up to the Fermi level. Considering the correlation of surface oxygen concentration with O $2p$ features in the valence bands, this observation demonstrates that the band-gap emission is

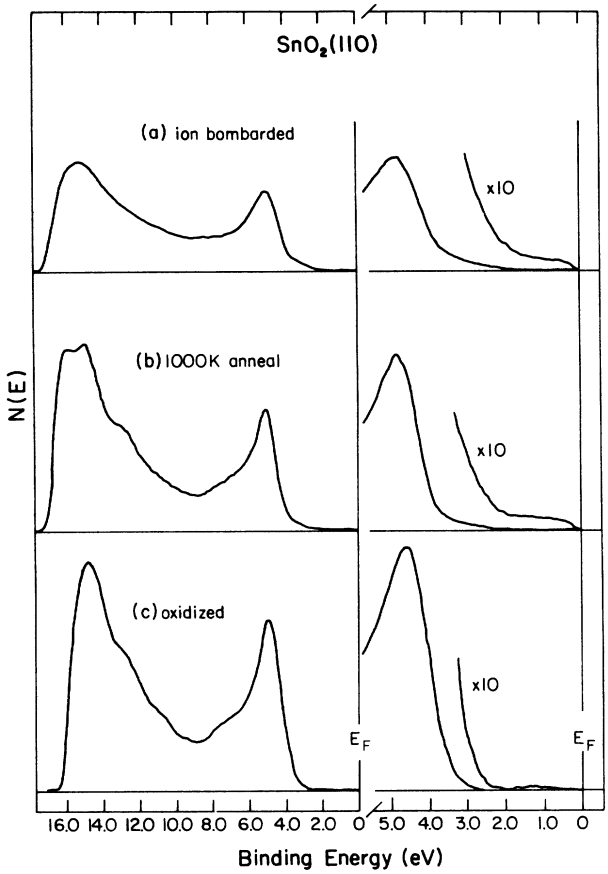

FIG. 2. UPS spectra obtained following three different surface preparations: (a) 2-keV ion bombardment, (b) ion bombarded and annealed in vacuum at 1000 K, and (c) oxidized in 1.0 Torr and O_2 at 700 K. The panels on the left are complete He I spectra while the right-hand panels are enlarged views of the band-gap regions and the tops of the valence bands. All spectra are referenced to the Fermi level.

associated with an oxygen deficiency at the surface as has been suggested previously.[2,9–12] Notice that the spectrum of the oxidized surface in Fig. 2 suggests only a very small density of states in the band gap, indicating that the oxidization process removes nearly all the surface oxygen deficiency. In other words, the lack of defect electronic states in the band gap indicates that the oxidized surface is stoichiometric. The oxidized surface is believed, therefore, to closely approximate an ideal, stoichiometric (110) surface (i.e., a surface terminated with bridging oxygens). However, the possibility of some low concentration of oxygen vacancies cannot be ruled out.

B. Preparation of an ideal surface

The removal of band-gap electronic states in UPS was one of the criteria used to determined the minimum conditions of oxygen pressure and temperature required to reproducibly prepare an ideal (i.e., completely oxidized) surface. The second criterion used was to monitor surface band bending with UPS. The positions of the bands, as determined from shifts in the valence-band edge, have

been found to be sensitive to small changes in surface composition.[23] Oxygen vacancies act as donors that result in the formation of an accumulation layer that causes downward band bending at the surface. Therefore, we also looked for oxidation conditions which shifted the bands as far up (i.e., to the lowest binding energies) as possible.

A number of different oxygen pressures ranging from 0.01 to 10.0 Torr were examined for the oxidation process using UPS. In all cases, a sample temperature of 700 K was used because it has been found to be sufficient to allow for surface atom mobility in the studies of thermally driven reconstructions.[4] Using the criteria discussed above it was found that complete oxidation occurs at 1 Torr and above. It was also found that variations in the oxidation time from 3 to 30 min at 1.0 Torr had no effect on the UPS spectra. Therefore, the oxidation conditions used throughout this work were 1.0 Torr of O_2 at 700 K for 3 min. Following oxidation, the sample was cooled to near room temperature in 1.0 Torr of oxygen before the chamber was evacuated. This cooling procedure was used because previous investigators have shown that heating an oxidized SnO_2 surface in vacuum removes surface lattice oxygen.[2] It is also worth noting that the measured conductivity following the oxidation procedure (see below) is near the reported value for the bulk. This suggests that the surface is well oxidized and that this preparation gives a truly flat-band condition (i.e., zero surface potential).

One final concern about the oxidation procedure was the possibility that adsorbed oxygen (as opposed to in-plane or bridging lattice oxygen) remained on the surface after the oxidation procedure.[24] We note that adsorbed O_2^{2-} has been identified recently on NiO single crystal surfaces[25] at room temperature in UHV. It was necessary to investigate this possibility since the presence of adsorbed oxygen would affect our ISS measurements of surface composition. In addition, Chang[26] has reported an EPR study of oxygen adsorption on tin oxide powder. He found that the amount of adsorbed oxygen (O_2^{1-} and O^{1-}) depended strongly on the oxygen partial pressure, but that some adsorbed oxygen could be observed even after heating the powder in vacuum. The primary species at room temperature was found to be molecular oxygen whether it was adsorbed molecularly below 375 K or converted from a high-temperature atomic form upon cooling from temperatures above 475 K. We feel that the observation of adsorbed oxygen under vacuum in the EPR study can be attributed to the poor vacuum (relative to our UHV chambers) attainable in the apparatus, and to the large concentration of surface defect sites which are inevitably available on a powder sample. Nevertheless, the EPR results indicate that molecular oxygen would be the most likely adsorbed species to be found under our experimental conditions.

Several experimental observations lead to the conclusion that no significant amount of adsorbed oxygen is present on the single-crystal sample in the UHV analysis chamber ($P < 10^{-10}$ Torr) at 300 K following the oxidation treatments. First, the shape of the O 1*s* spectrum in XPS reveals no broadening after the oxidation treatments. If adsorbed oxygen were present, broadening would be expected. Indeed, such broadening was observed for O_2 adsorption on NiO (Ref. 25) and during the oxidation of a number of different metals.[27] Second, an examination of differences in the UPS valence-band spectra before and after oxidation shows no structure consistent with either adsorbed molecular or atomic oxygen.[25,27] In fact, the oxidation treatment results in an increased intensity over the entire valence band range. Since there are O 2*p* contributions throughout the valence bands, this observation suggests that oxygen has been incorporated as lattice oxygen rather than adsorbed oxygen. Third, it has also been found that heating the oxidized surface at a temperature as low as 400 K removes a small amount of surface oxygen and results in the formation of a small density of defect states in the band gap (to be shown below). This observation indicates that the first oxygen removed by heating in vacuum is lattice oxygen and not adsorbed oxygen.

C. Thermal production of oxygen vacancies

1. "Bridging" oxygen vacancies

A sequence of ISS experiments was performed as a preliminary examination of the extent of surface reduction due to vacuum annealing, and as a final check on the possible effects due to adsorbed oxygen. Figure 3 shows the ISS spectra obtained following three sample pretreatments: (a) cleaned by ion bombardment then heated at 1000 K in vacuum to ensure a well ordered (1×1) surface, followed by oxidation as described above; (b) heating the oxidized surface at 1000 K in UHV for 3 min; and (c) exposure to 1 Torr of O_2 for 3 min at room temperature following treatments (a) and (b). Note that under these different preparation conditions the surface always displays a (1×1) LEED pattern characteristic of the bulk periodicity. In each spectrum the oxygen signal appears at a relative energy (E/E_0) of 0.44, and the tin signal appears at 0.90. The oxidized surface [Fig. 3(a)] exhibits the

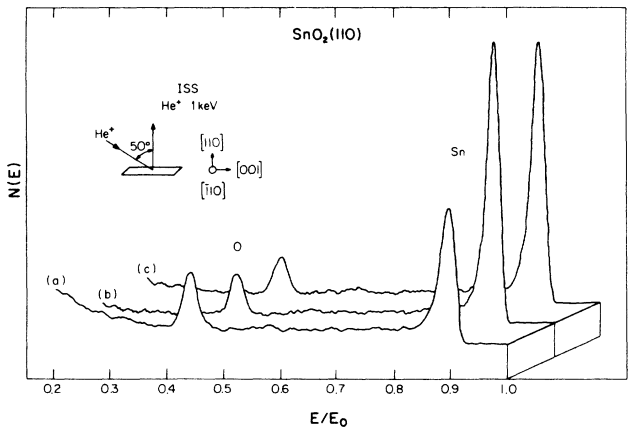

FIG. 3. ISS spectra following (a) oxidation, (b) heating to 1000 K in vacuum following treatment (a), and (c) exposure to 1 Torr of O_2 for 3 min at room temperature following treatment (b).

largest oxygen signal and the smallest tin signal. Heating the oxidized surface to 1000 K in UHV [Fig. 3(b)] decreases the oxygen signal somewhat, but results in a doubling of the tin peak height. Exposing the surface characterized by Fig. 3(b) to 1 Torr of O_2 at 300 K results in only a small decrease in the tin signal and little change in the oxygen signal as shown by Fig. 3(c).

The decrease in oxygen and increase in tin signal for the vacuum-annealed surface [Fig. 3(b)] versus the oxidized surface [Fig. 3(a)] suggests two possible processes: (1) the desorption of oxygen from the surface, or (2) the migration of tin from the bulk to the surface. Several observations rule out the migration of tin to the surface. Tin migration would require a source of excess tin in the bulk, which might be present if the material underwent some bulk reduction as a result of annealing in vacuum. However, cycles of ion bombardment and heating during the course of these experiments led to reproducible trends in the electronic properties as a function of annealing temperature. The sample conductivity and the position of E_F with respect to the valence bands (as determined by UPS) were stable for a given annealing temperature following these treatments, and did not show any long-term variation indicative of a bulk reduction. Note that, experiments with deposited tin on the $SnO_2(110)$ surface indicate up to a 40-fold increase in sample conductivity for coverages near 0.1 monolayer.[28] Conductivity measurements reported below (Sec. IV C 2) for annealing treatments of the oxidized surface show only small changes in the temperature range associated with the largest decrease in the [O]/[Sn] ratio as measured by ISS. Therefore, it is concluded that the difference between Figs. 3(a) and 3(b) is caused by oxygen desorption.

The large room-temperature oxygen exposure (about 10^8 L) associated with Fig. 3(c) mimics the oxygen exposure seen by the sample during the cooling phase of the oxidation procedure. [1 langmuir (L)$\equiv 10^{-6}$ Torr sec.] Because the interconversion of adsorbed oxygen between the molecular and atomic forms was found to be a reversible function of temperature in the ESR experiments of Chang,[26] the form of any adsorbed species should depend only on the final temperature before evacuation. The lack of significant change between Figs. 3(b) and 3(c) indicates once again that the amount of adsorbed oxygen is small, and has little effect on the surface composition as probed by ISS. The oxygen desorbed by heating in vacuum must therefore be lattice oxygen (e.g., bridging or in-plane) which is incorporated into the surface under the high-temperature oxidation conditions.

Based on AES measurements, deFrésart and coworkers[3] have proposed that a $SnO_2(110)$-1×1 surface prepared by ion bombardment and heating in vacuum is terminated nominally by a tin and oxygen containing plane, which is equivalent to removing completely the top layer of bridging oxygens from an ideal surface. A similar proposal has been made by P. A. Cox and coworkers[2] based on an XPS study of polycrystalline tin-oxide materials. Modeling their XPS data with an ideal $SnO_2(110)$ surface, they suggest that bridging oxygen anions are easily removed from an oxidized surface by heating in vacuum. The ISS data in Fig. 3(a) for the oxidized surface and Fig. 3(b) for the vacuum annealed surface are *direct* evidence supporting this proposal.

Figure 4 shows two ball model illustrations of the $SnO_2(110)$ surface based on the ionic radii of Sn^{4+} and O^{2-} ions and assuming no surface relaxation. The illustrations in Fig. 4 are aligned such that the surface is viewed along the [001] direction at an angle of 50° with respect to the surface normal. Figure 4(a) illustrates a (nearly) ideal surface terminated by bridging oxygens. A few bridging oxygen vacancies have been "created" in the surface to reveal the rows of (ideally) sixfold-coordinated tin cations hidden underneath. Figure 4(b) illustrates the results of stripping away the plane of bridging oxygens from an ideal surface. A few in-plane oxygen vacancies are also included in this view. As mentioned above (Sec. II), no experimental data is available from which to determine the degree of relaxation that may occur near a vacancy. Note that all the visible tin cations in Fig. 4(b) (away from the front edge of the crystal) are in the same atomic plane. The perspective shown in Figs. 4(a) and 4(b) is along the incident ion-beam direction used in the ISS measurements; in effect, Fig. 4 illustrates what the ion beam "sees" of the crystal. In Fig. 4(a) the bridging

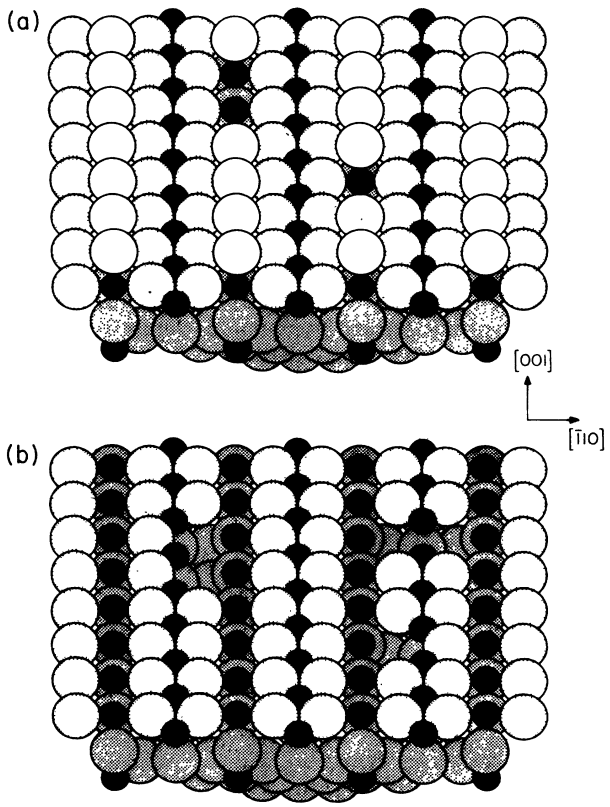

FIG. 4. Ball model illustration of the surface viewed along the direction of the incident ion beam in the ISS experiments. View (a) shows a nearly perfect (110) surface while view (b) shows a "bare" surface following the removal of all top-layer bridging oxygens. A few "in-plane" oxygen vacancies are also shown in (b). These illustrations are schematic, and are not meant to imply that relaxation does not occur near the vacancies.

oxygen anions completely obscure ("shadow") the sixfold coordinated tin cations. By stripping away the full layer of bridging oxygens, the available number of surface tin atoms that can be sampled with ISS increases by a factor of two, in agreement with the doubling of the tin peak height observed when the oxidized surface is heated in vacuum [Figs. 3(a) and (3b)]. Because of the large scattering cross section for tin relative to oxygen, this effect is illustrated most dramatically by the increase in the tin signal rather than a smaller relative decrease in the oxygen signal. Note that surface atom shadowing effects in ISS such as those illustrated here are well documented.[29,30]

It should be pointed out that the rather remarkable agreement between the factor-of-two increase in exposed tin cations and the factor-of-two increase in tin peak height in ISS is to some degree fortuitous. A comparison of the integrated scattering signal (rather than peak heights) from tin in these two cases shows an increase of more like a factor of 2.65. However, from Fig. 4(b) it can be seen that the exposed geometric cross-sectional area of the fourfold-coordinated cations (i.e., those exposed by removing the rows of bridging oxygens) is significantly larger than the exposed cross-sectional area of the fivefold-coordinated cations. If one assumes that the scattering cross section for a given atom type is directly proportional to its exposed geometric cross section, an increase in tin signal by 2.63 times would be predicted, representing an agreement of better than 1%. This agreement is most likely also fortuitous, but the comparisons have been belabored to stress the structural and compositional sensitivity of the ISS measurements. A true prediction of the variation in tin signal would require a precise knowledge of the repulsive interaction potential between the incident He ion and the different surface species, as well as information about the effects of surface condition on the neutralization probability. These data are not presently available. However, we feel that the UPS and ISS data presented in Figs. 2 and 3 demonstrate conclusively that (1) the *in situ* oxidation procedure gives an ideal, stoichiometric $SnO_2(110)$ surface, (2) heating to sufficiently high temperatures in vacuum removes the layer of bridging oxygens from an ideal surface, and (3) little or no interference from adsorbed oxygen species affects the observations.

A systematic study also was performed with ISS of the variation of surface composition for an oxidized surface with annealing temperature. It was found during this investigation that the [O]/[Sn] ratio measured by ISS was sensitive to the He^+ dose during the measurement. He^+ ions at 1 keV were found to remove oxygen easily from an oxidized surface. To minimize this effect, small ion-beam currents (10 nA) were used and spectra were taken rapidly over small energy ranges, first for the oxygen signal and then for the tin signal. Lastly, a third spectrum was also taken over the entire range of relative energy (such as those shown in Fig. 3) to ensure that no unusual multiple-scattering or impurity effects were observed. A comparison between two successive data sets (three spectra per data set) showed variations of 10–15% in the [O]/[Sn] ratio for an oxidized surface due to sputtering of oxygen during the measurements. Sputtering effects were less significant on surfaces which exhibited an oxygen deficiency at the outset. Figure 5 shows the ISS [O]/[Sn] ratio for an oxidized surface (top curve) and an ion-sputtered surface (bottom curve) as a function of annealing temperature. The data are normalized to the [O]/[Sn] ratio for an oxidized surface. While examining the effects of annealing on the oxidized surface, the sample was oxidized and then heated to the appropriate temperature *prior to each measurement* to ensure that no ion-beam effects were carried over to subsequent data points. A comparison of the two curves in Fig. 5 emphasizes the wide variability in surface oxygen concentration first pointed out in Table I.

The two dashed lines in Fig. 5 indicate simple, theoretical estimates of the composition ratios that would be produced by complete removal of the top layer of bridging oxygens from an ideal surface. The top line at 0.33 is based on the assumption of equal cross sections for bridging and in-plane oxygen anions and equal cross sections for fourfold- and fivefold-coordinated tin cations. The lower line at 0.27 accounts for variations in the viewed geometric cross sectional area of the two different oxygen species and the two different tin species. Note that these two lines *do not* define limiting values for top-layer oxygen removal. In view of the lack of information available about variations in the scattering cross sections, the lines merely represent expected values under two different sets of simplifying assumptions. One assumption inherent to both cases is that the oxidation treatment yields an ideal surface terminated with a full layer of bridging oxygen atoms.

2. *"In-plane" oxygen vacancies*

From Fig. 5 it is clear that heating an ideal surface in vacuum removes a large fraction of surface bridging oxy-

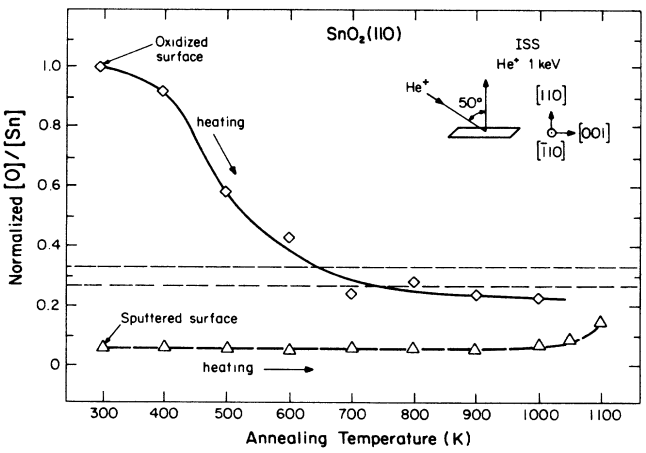

FIG. 5. Variation in the normalized ISS [O]/[Sn] ratio with annealing temperature in vacuum for an oxidized surface (upper solid curve) and an ion-bombarded surface (lower dashed curve). The two dashed lines at 0.33 and 0.27 represent the expected compositions under two different sets of simplifying assumptions (see text for discussion) equivalent to complete removal of the top layer of bridging oxygen atoms from an oxidized surface.

gens at temperatures as low as 500 K. Higher-temperature treatments (700 K and above) have only a small effect on the measured composition. The [O]/[Sn] ratios for the data from 700 to 1000 K suggest the removal of more than just the layer of bridging oxygens, implying the possible removal of some in-plane oxygens as well. However, the lines describing the limit of top layer (bridging oxygen) removal are only estimates, so that values slightly below these lines are not necessarily strong evidence for the removal of in-plane oxygen atoms. Notice in Fig. 4(b) that removal of a small number of in-plane oxygen atoms should have only a small effect on the composition measured with ISS since the next two atomic layers are composed entirely of oxygen anions (see also Sec. II). However, a high concentration of in-plane oxygen vacancies would be expected to decrease the [O]/[Sn] ratio significantly because of an increase in the viewed geometric cross-sectional area associated with changing a fivefold-coordinated cation to a fourfold coordination [Fig. 4(b)]. Examination of the data from annealing the sputtered surface in vacuum (bottom curve) shows significantly lower [O]/[Sn] ratios than observed for similar treatments of the oxidized surface. The sputtered surface undergoes a number of different reconstructions as a function of annealing temperature,[3,4] but the data shown at the higher temperatures of about 1000 K are characteristic of a (1×1) surface. These data indicate that the $SnO_2(110)$ surface can support an oxygen deficiency larger than that expected for a "bare" surface (i.e., a surface with the layer of bridging oxygens removed), while still maintaining a (1×1) LEED periodicity. The possibility of forming in-plane oxygen vacancies is therefore highly likely. Supporting evidence for the formation of in-plane oxygen vacancies is given by conductivity measurements (next paragraph) and gas adsorption data (Sec. IV E) as discussed below.

Figure 6 shows a comparison between variations in surface composition (from the ISS data in Fig. 5) and the change in electrical conductivity for heating an oxidized surface in vacuum. All conductivity measurements were made after the sample cooled to 300 K. The change in conductivity is small for annealing temperatures up to 700 K. As can be seen from the ISS measurements, this temperature range is associated with the removal of the top layer of bridging oxygens, i.e., the formation of a "bare" surface. The removal of bridging oxygen atoms therefore has only a relatively small effect on the surface conductivity. However, annealing at higher temperatures causes a much larger increase in the conductivity. The observed change in conductivity indicates that something other than bridging oxygen vacancies are formed at temperatures above 700 K. Since the bulk material exhibited stability to vacuum heat treatments during the course of these experiments, the observed conductivity changes must be dominated by surface effects. Because surface oxygen vacancies are known to act as n-type donors,[3,5] the conductivity increase is assigned to the formation of a second type of oxygen vacancy (i.e., something other than a bridging oxygen vacancy). The most likely alternative is that in-plane oxygen vacancies are formed at the higher annealing temperatures. It should be noted that the ISS data give no conclusive evidence for the formation of in-plane oxygen vacancies. In fact, in the absence of any identifiable shadowing or multiple scattering effects, it is impossible to make such a distinction with ISS, particularly in view of the small change observed in the [O]/[Sn] ratio above 700 K. However, the observed conductivity changes are clear evidence for the formation of a second type of surface defect.

D. Oxygen vacancy electronic properties

The two regimes in the conductivity curve shown in Fig. 6 indicate significantly different electronic properties for the in-plane and bridging vacancies. Therefore, UPS was used to study the surface electronic structure following annealings of an oxidized surface. Fig. 7 shows the variations in work function, band bending, and electron affinity for the oxidized surface as a function of annealing temperature. Work-function changes, $\Delta\phi$, were found from variations in the width of the UPS spectra. Surface band bending changes, $e\,\Delta V_s$, where V_s is the surface po-

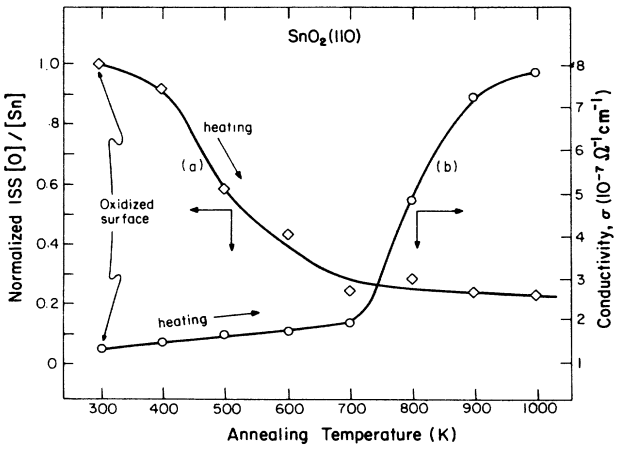

FIG. 6. Comparison between variations in the normalized ISS [O]/[Sn] ratio and the conductivity for an oxidized surface as a function of vacuum annealing temperature.

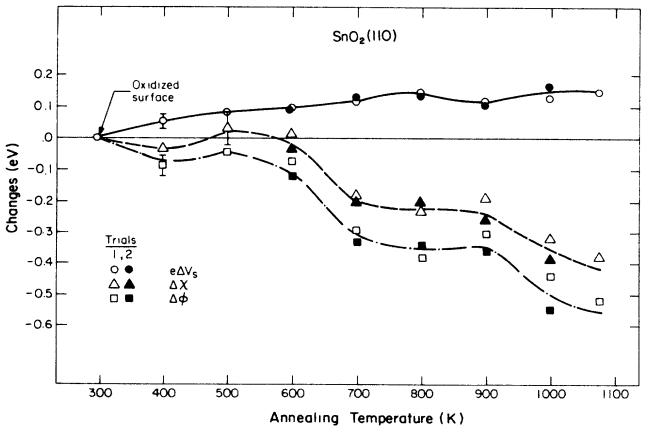

FIG. 7. Variation in work function, $\Delta\phi$, band bending, $e\,\Delta V_s$, and electron affinity, $\Delta\chi$, upon heating an oxidized surface in vacuum. Work-function and band-bending changes were determined from UPS at 300 K. Electron-affinity changes were calculated from $\Delta\phi$ and $e\,\Delta V_s$.

tential and e is the electron charge, were found from shifts of the low-binding-energy edge of the valence-band emission in UPS. Variations in electron affinity, $\Delta\chi$, were then calculated from the relationship

$$\Delta\chi = \Delta\phi + e\,\Delta V_s$$

where a positive surface potential implies downward band bending.

From Fig. 7 it is apparent that the surface potential increases as oxygen is removed by heating in vacuum. The positive change in surface potential (i.e., downward band bending) indicates the formation of an accumulation layer caused by defect donor states.[31] This observation is consistent with the formation of oxygen vacancies (as discussed above) which act as n-type donors.[3-7] Also in Fig. 7, it is seen that the work function generally decreases as a function of annealing temperature. The change in electron affinity which describes changes in the surface dipole layer also shows the same general trend of a decrease with increased annealing temperature. Both of these trends are consistent with the removal of surface oxygen by heating in vacuum.

Changes in the band gap (defect state) emission are shown in Fig. 8 for the oxidized surface as a function of vacuum annealing temperature. The data in Fig. 8 are UPS difference curves. In each case the spectrum for the oxidized surface has been subtracted from the spectrum taken after the heat treatment. The difference curves are referenced to the CBM by using the calculated position of the Fermi level in the bulk (0.53 eV below the CBM) and assuming a flat band situation (i.e., zero surface potential) for the oxidized (ideal) surface.[32,33] Before taking the differences, the spectra were shifted to account for changes in band bending. It is worth noting that the shapes of the curves were not sensitive to the alignment used to correct for band bending, although some small variations in intensity were found.

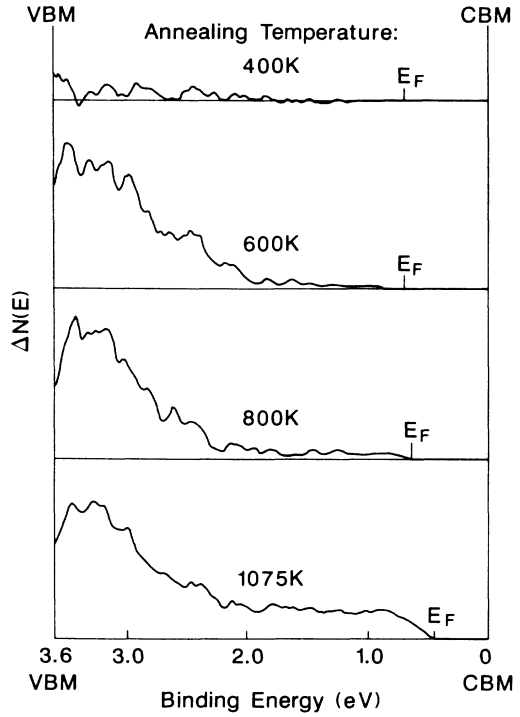

FIG. 8. UPS difference curves showing the increase in band-gap (defect) electronic states caused by heating an oxidized surface in vacuum. The curves are referenced to the conduction-band minimum (CBM).

From Fig. 8 it is observed that the lower-temperature vacuum anneals (below 700 K) result in the formation of occupied states in the gap which overlap the VBM. These states appear in the temperature range associated with the removal of bridging oxygen atoms from the ideal surface, and may therefore be associated with bridging oxygen vacancies. The formation of these bridging vacancies lowers the coordination number of half the surface tin cations from an initial value of six (the bulk coordination) to four. The remaining surface tin cations maintain a fivefold coordination just as on an ideal surface. These results confirm the hypotheses of P. A. Cox and co-workers who observed similar effects on polycrystalline samples.[2] Using the (110) surface as a model, they suggested that the appearance of band gap states near the VBM should be due to the removal of bridging oxygen anions. Based on the solid-state chemistry of Sn^{2+} compounds, they argued that the four-fold coordinated cations are reduced from a Sn^{4+} to a Sn^{2+} charge state, and that the defect states near the VBM are Sn $5s-5p$ lone-pair hybrids occupying stereochemical positions in the structure.[34] By reducing half the cations at the "bare" surface (i.e., all bridging oxygens removed) to a Sn^{2+} charge state, the surface maintains charge neutrality which could account for the stability of this highly nonideal surface. At this point, note that it is not possible to distinguish between Sn^{2+} and Sn^{4+} cations with either XPS or AES.[35-37]

As seen from Fig. 8, heating to temperatures above 700 K results in the appearance of states higher in the gap which extend up to the Fermi level. The emission from these states is very weak for annealing temperatures around 800 K, the critical temperature range where the conductivity begins to increase, but is easily observed in the difference spectra for higher (>900 K) annealing temperatures. These additional band-gap states extend over a binding energy range of more than 1 eV, and therefore cannot be due merely to instrumental broadening (the analyzer resolution is 0.15 eV) or improper band alignment in correcting for band bending changes (the maximum reported band-bending shift is less than 0.15 eV). Also, occupied states near the Fermi level are very active as n-type donors, and by comparison to Fig. 6 it is seen that the appearance of these additional states high in the gap accompanies the large increases in conductivity. The conductivity measurements probe changes in the conduction band free carrier density which are too small to observe with UPS, but the occupied states high in the gap which are observable with UPS may be associated with nonionized donor levels which, when ionized, can give rise to the increase in free carriers. We attribute these defect electronic states to in-plane oxygen vacancies. The small variation in the [O]/[Sn] ratio in ISS observed for the oxidized surface in this temperature range suggests a

low concentration of in-plane vacancies, consistent with the idea of isolated defects. The formation of a random, isolated in-plane oxygen vacancy lowers the coordination number of one adjacent surface tin cation from four to three, while the other two nearest neighbors go from a fivefold to a fourfold coordination. If the threefold-coordinated cation is considered to be in a 2+ oxidation state (as suggested by P. A. Cox *et al.*[2]) *prior* to the removal of the in-plane oxygen, a two-electron transfer from an in-plane vacancy to this cation would result in a metallic (Sn^0) surface tin atom. However, no detectable metallic tin signal was observed in XPS. (Note that while Sn^{2+} and Sn^{4+} cannot be distinguished with XPS, metallic tin may be easily distinguished from cationic tin.) If one assumes that the concentration of threefold-coordinated cations is not below the detection limit, the absence of a metallic tin feature in XPS suggests that the two electrons associated with the in-plane oxygen vacancy must be bound, at least in part, to the two remaining fourfold-coordinated nearest-neighbor tin cations. (Note also that even for surfaces prepared by ion bombardment and vacuum annealing which are measurably more oxygen deficient, no metallic tin signal is observed in XPS.) The possibility of a one-electron transfer to each of the two fourfold-coordinated cations is ruled out since no Sn^{3+} compounds are known.[34] We suggest, therefore, that the two electrons are bound in a surface color center to maintain local charge neutrality. The missing oxygen anion is equivalent to a localized positive charge in the lattice which binds the two vacancy electrons by its Coulombic field. This picture suggests that the charge is localized around the in-plane vacancy in a nonionized surface donor state.

The large energy width (over 1 eV) of the states associated with these vacancies formed at high temperatures is not well understood. If the electronic states are indeed associated with random, isolated vacancies as described above, band dispersion is not a reasonable explanation. One possible explanation is the existence of the donor state in several different electronic configurations (neutral, singly charged, doubly charged) controlled by occupation statistics. Another explanation could be the existence of geometrically inequivalent sites due to the formation of isolated and adjacent vacancies (possibly a divacancy?), or sites experiencing differing degrees of relaxation. The data presented above does not distinguish between these possibilities, thus leaving the explanation open to speculation.

E. Interaction of oxygen with defect electronic states at 300 K

The idea of two distinct types of surface oxygen vacancies (bridging and in-plane) gains further support when one examines the interaction of oxygen at room temperature with an *oxygen-deficient* surface. Figure 9 shows a UPS difference curve for a 10^5 L oxygen dose on an oxygen deficient surface. The adsorption experiments were carried out on a (1×1) surface prepared by ion bombardment and heating to 1000 K in vacuum. The band-gap emission in UPS for a surface prepared in this way is indistinguishable in shape from a surface prepared by oxidation and annealing to 1000 K in vacuum. However, the surface produced in this manner is, in fact, more oxygen deficient (see ISS results in Fig. 5), and also has a larger density of states in the band gap. This particular preparation was chosen because, in general, the $SnO_2(110)$ surface is fairly unreactive during UHV gas exposures,[23] and the higher oxygen deficiency results in a change following adsorption which is easier to distinguish in UPS. As mentioned above, this surface preparation appears to produce a higher concentration of in-plane oxygen vacancies than found on the oxidized and vacuum annealed surface. A typical conductivity of a surface following this preparation is $2.5\times10^{-6}\ \Omega^{-1}\,cm^{-1}$, a factor of 3 higher than observed on the oxidized and annealed surface.[5]

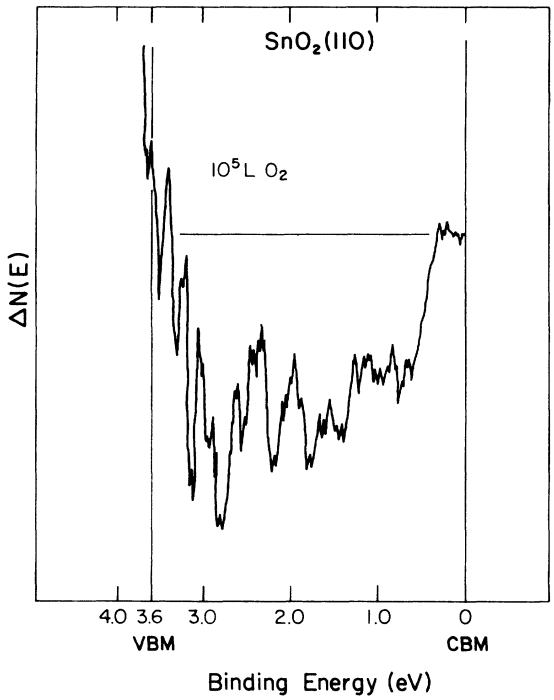

FIG. 9. UPS difference curves illustrating adsorbate-induced changes in the band-gap density of states for an ion-bombarded, vacuum-annealed 1×1 surface following exposure to 10^5 L of O_2.

Figure 9 demonstrates that O_2 exposures decrease the emission throughout the band gap, indicating a reaction of oxygen with both types of defect electronic states. This behavior supports the idea that the observed electronic states are both due to oxygen vacancies. Likewise, the decrease throughout the gap is an indication that the defect electronic states formed by ion bombardment and annealing, because of their susceptibility to gas-phase oxygen at low temperature and pressure, are due, at least partially, to true *surface* defects. The low mobility of oxygen through the SnO_2 lattice (indicated by the lack of bulk reduction and the inability to form a nearly completely oxidized surface by simply heating in vacuum[4]) suggests that room-temperature oxygen adsorption would not result in a significant depopulation of states associat-

ed with subsurface oxygen vacancies. Note that theoretical studies of the band structure of oxygen deficient $TiO_2(110)$ surfaces (a material with the same structure) have suggested that *subsurface* rather than surface oxygen vacancies are responsible for the appearance of band gap electronic states.[38] However, similar calculations for $SnO_2(110)$ failed to predict the ocurrence of band-gap electronic states associated with any type of oxygen vacancy.[16] It should be noted that our experimental results clearly demonstrate the existence of band-gap electronic states associated with *surface* oxygen vacancies, but do not rule out the possible existence of *subsurface* oxygen vacancies.

The difference curve in Fig. 9 indicates that less than a 20% decrease in the band-gap emission occurs when the defect 1×1 surface is exposed to oxygen. If the possible existence of subsurface oxygen vacancies is neglected, this small decrease would mean that the majority of surface oxygen vacancies are not affected by the room-temperature O_2 dose. Similar results were found with ISS [Fig. 3(c), Sec. IV C 1] when checking for the presence of adsorbed oxygen following the procedure used to prepare an ideal surface. In that case, the reaction of oxygen at bridging vacancies was found to be limited at room temperature even after a 1 Torr exposure totaling about 10^8 L. Since complete oxidation can be accomplished under similar conditions at elevated temperature (700 K), the oxygenation process must be activated. The ESR results of Chang[26] illustrate that tin oxide does not dissociate O_2 effectively at room temperature, but supports atomic oxygen (O^{-1}) as the primary adsorbed oxygen species above 475 K. Therefore, the activation barrier observed with the oxidation process is probably associated, at least in part, with the dissociation of adsorbed oxygen from a molecular to an atomic form.

V. SUMMARY AND CONCLUSIONS

The structural and electronic properties of the (1×1) periodicity of ideal and oxygen deficient $SnO_2(110)$ surfaces have been studied in detail. Using a variety of complementary techniques (XPS, ISS, LEED, UPS and conductivity measurements), it was found that a nearly ideal $SnO_2(110)$ surface could be prepared by an *in situ* oxidation treatment at 700 K in 1 Torr of O_2. Using ISS and UPS, it was conclusively demonstrated that heating this ideal surface in vacuum at temperatures below 800 K led to defect states in the band gap near the VBM which arise from bridging oxygen vacancies, i.e., a reduction of sixfold-coordinated Sn^{+4} cations on the ideal surface to a fourfold coordination. The tin cations resulting from this reduction can reasonably be described as Sn^{+2} species as earlier suggested by P. A. Cox and co-workers.[2] Heating at temperatures of 800 K and above led to the creation of additional states higher in the gap which are accompanied by a significant increase in surface conductivity. It has been argued that these states are associated with the formation of in-plane oxygen vacancies which result in threefold and fourfold-coordinated tin cations. Electronically, the in-plane oxygen vacancies are thought to be best described as surface color-center-like defects. Gas adsorption experiments with oxygen at room temperature demonstrated that the defect electronic states in the band gap can be associated with surface rather than subsurface oxygen vacancies.

The behavior demonstrated by the $SnO_2(110)$-1×1 surface in terms of sequential removal of different surface oxygen species as a function of temperature makes this an ideal system for which to identify and characterize different types of oxygen vacancies. We note that a great deal more work has been done on the characterization of TiO_2 single crystal surfaces (for example, see Ref. 1 and references therein), especially the (110) surface which is structurally identical to the $SnO_2(110)$ surface. To our knowledge, ISS has not been used to characterize the $TiO_2(110)$ surface. Such an investigation might prove as useful on $TiO_2(110)$ as it has on $SnO_2(110)$. However, the ease of interpretation may be lost if several different vacancies are formed under similar conditions, or if the mobility of oxygen through the lattice is sufficient to keep the surface in a "well oxidized" condition.

ACKNOWLEDGMENTS

The authors wish to thank to Professor R. Helbig for supplying the single crystal used in this study, and Dr. J. W. Erickson for his work on the four-point conductivity measurements. Thanks go also to G. Scace for technical assistance. Two of us (D.F.C. and T.B.F.) gratefully acknowledge the support of the National Bureau of Standards—National Research Council Postdoctoral Program.

*Permanent address: Department of Chemical Engineering, Virginia Polytechnic Institute and State University, Blacksburg, VA 24061-6496.

[1]V. E. Henrich, Rep. Prog. Phys. **48**, 1481 (1985).
[2]P. A. Cox, R. G. Egdell, C. Harding, W. R. Patterson, and P. J. Tavener, Surf. Sci. **123**, 179 (1982).
[3]E. deFrésart, J. Darville, and J. M. Gilles, Appl. Surf. Sci. **11/12**, 637 (1982); Solid State Commun. **37**, 13 (1980).
[4]D. F. Cox, T. B. Fryberger, S. Semancik, and P. D. Szuromi (unpublished).
[5]J. Erickson and S. Semancik, Surf. Sci. **187**, L658 (1987).
[6]C. G. Fonstad and R. H. Rediker, J. Appl. Phys. **42**, 2911 (1971).
[7]S. Samson and C. G. Fonstad, J. Appl. Phys. **44**, 4618 (1973).
[8]P. L. Goody and G. J. Lapeyre, *Physics of Semiconductors: Proceedings of the 13th International Conference on Semiconductor Physics* (North-Holland, New York, 1976), p. 150; P. L. Gobby, Ph.D. dissertation, Montana State University, 1977, University Microfilms International, Ann Arbor, MI.
[9]R. G. Egdell, S. Erickson, and W. R. Flavell, Solid State Commun. **60**, 835 (1986).
[10]D. F. Cox, S. Semancik, and P. D. Szuromi, J. Vac. Sci. Technol. A **4**, 627 (1986).
[11]D. F. Cox, T. B. Fryberger, J. W. Erickson, and S. Semancik,

J. Vac. Sci. Technol. A **5**, 1170 (1988).
[12]S. Semancik and D. F. Cox, Sensors and Actuators **12**, 101 (1987).
[13]F. J. Arlinghaus, J. Phys. Chem. Solids **35**, 931 (1974).
[14]J. L. Jacquemin and G. Bordure, J. Phys. Chem. Solids **36**, 1081 (1975).
[15](a) J. Robertson, J. Phys. C **12**, 4767 (1979); (b) Phys. Rev. B **30**, 3520 (1984).
[16](a) S. Munnix and M. Schmeits, Solid State Commun. **43**, 867 (1982); (b) Surf. Sci. **126**, 20 (1983); (c) Phys. Rev. B **27**, 7624 (1983); (d) Phys. Rev. B **33**, 4136 (1986).
[17]B. Thiel and R. Helbig, J. Cryst. Growth **32**, 259 (1976).
[18]P. Türkes, Ch. Pluntke, and R. Helbig, J. Phys. C **13**, 4941 (1980).
[19]J. W. Erickson and S. Semancik, J. Vac. Sci. Technol. A **5**, 115 (1987).
[20]T. E. Madey and J. T. Yates, Jr., Surf. Sci. **63**, 203 (1977).
[21]S. Semancik and D. F. Cox, J. Vac. Sci. Technol. A **4**, 626 (1986).
[22]W. Göpel, G. Rocker, and R. Feierabend, Phys. Rev. B **28**, 3427 (1983); W. Göpel, J. A. Anderson, D. Frankel, M. Jaehnig, K. Phillips, J. A. Schäfer, and G. Rocker, Surf. Sci. **139**, 333 (1984).
[23]D. F. Cox, T. B. Fryberger, J. W. Erickson, and S. Semancik (unpublished).
[24]The possibility of interference from water contamination during the oxygen exposures has been dismissed because the *oxidized* surface has been found to be nearly inert to water exposures as high as 10^8 L (Ref. 23).
[25](a) J. M. McKay and V. E. Henrich, Phys. Rev. B **32**, 6764 (1985); (b) J. Vac. Sci. Technol. A **5**, 722 (1987).
[26]S. C. Chang, J. Vac. Sci. Technol. **17**, 366 (1980).
[27]K. Wandelt, Surf. Sci. Rep. **2**, 1 (1982).
[28]J. W. Erickson, T. B. Fryberger, and S. Semancik, J. Vac. Sci. Technol. A **6**, 1593 (1988).
[29]E. P. Th. M. Suurmeijer and A. L. Boers, Surf. Sci. **43**, 309 (1973).
[30]H. H. Brongersma, J. Vac. Sci. Technol. **11**, 231 (1974).
[31]A. Many, Y. Goldstein, and N. B. Grover, *Semiconductor Surfaces* (Wiley, New York, 1965).
[32]To calculate the position of the Fermi level in the bulk at 300 K, a value of $10^{-7}\ \Omega^{-1}\,\mathrm{cm}^{-1}$ was used for the bulk conductivity (from Ref. 18), a value of 200 $\mathrm{cm}^2\,\mathrm{V}^{-1}\,\mathrm{sec}^{-1}$ was used for the mobility (from Ref. 6), along with an effective mass of $0.275m_e$ (from Ref. 33).
[33]K. J. Button, C. G. Fonstad, and W. Dreybrodt, Phys. Rev. B **4**, 4539 (1971).
[34]See for example A. F. Wells, *Structural Inorganic Chemistry*, 4th ed. (Clarendon, Oxford, 1975), p. 935.
[35]C. L. Lau and G. K. Wertheim, J. Vac. Sci. Technol. **15**, 622 (1978).
[36]R. A. Powell, Appl. Surf. Sci. **2**, 397 (1979).
[37]D. F. Cox and G. B. Hoflund, Surf. Sci. **151**, 202 (1985).
[38]S. Munnix and M. Schmeits, Phys. Rev. B **31**, 3369 (1985).

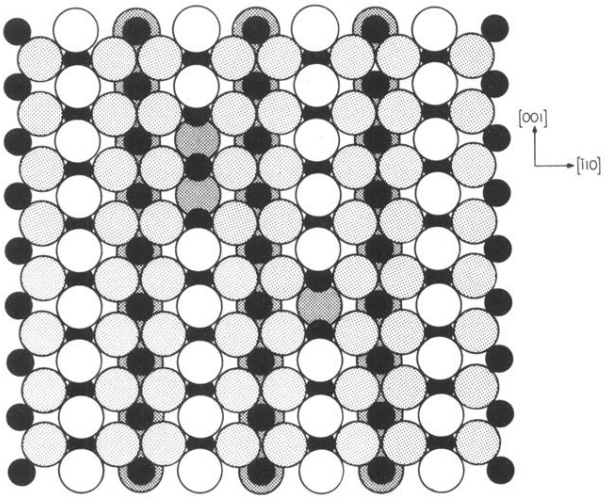

FIG. 1. Ball model illustration of a nearly perfect (ideal) $SnO_2(110)$ surface based on the ionic radii of the ions. The small solid circles represent Sn^{4+} cations, while the large open circles represent O^{2-} anions. All the visible tin cations are in the second atomic layer. Increased shading of the oxygen anions represents increased depth away from the surface. Several "bridging" oxygen anions have been removed from the terminal layer to represent oxygen vacancies and to give a clearer view of the (normally) sixfold-coordinated tin cations in the second layer.

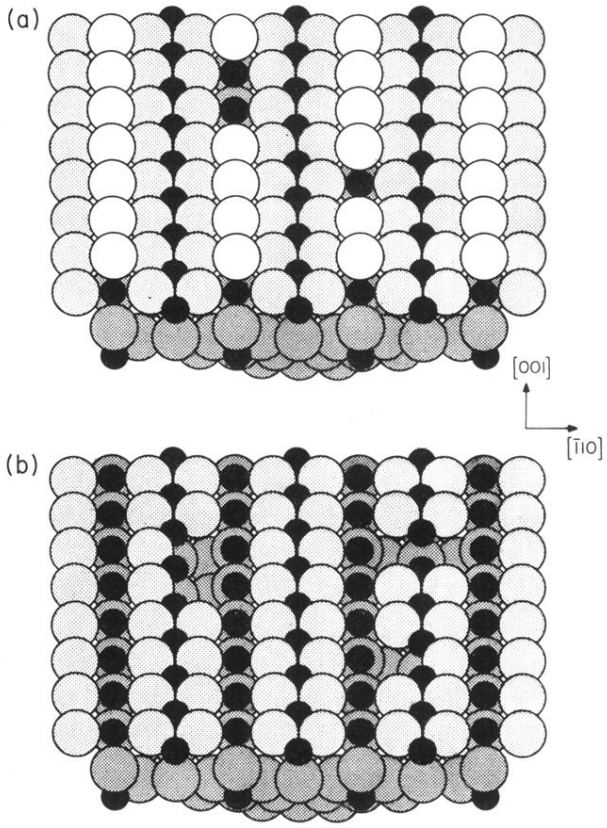

FIG. 4. Ball model illustration of the surface viewed along the direction of the incident ion beam in the ISS experiments. View (a) shows a nearly perfect (110) surface while view (b) shows a "bare" surface following the removal of all top-layer bridging oxygens. A few "in-plane" oxygen vacancies are also shown in (b). These illustrations are schematic, and are not meant to imply that relaxation does not occur near the vacancies.